Journal of the Endocrine Society, 2022, **6**, 1–10
https://doi.org/10.1210/jendso/bvac062
Advance access publication 12 April 2022
Research Article

CYP21A2 Gene Expression in a Humanized 21-Hydroxylase Mouse Model Does Not Affect Adrenocortical Morphology and Function

Tina Schubert[1], Nicole Reisch[2], Ronald Naumann[3], Ilka Reichardt[4], Dana Landgraf[1], Friederike Quitter[1], Shamini Ramkumar Thirumalasetty[1], Anne-Kristin Heninger[4,5], Mihail Sarov[4], Mirko Peitzsch[6], Angela Huebner[1], and Katrin Koehler[1]

[1]Children's Hospital, Medizinische Fakultät Carl Gustav Carus, Technische Universität Dresden, 01307 Dresden, Germany
[2]Medizinische Klinik und Poliklinik IV, Ludwig-Maximilians-Universität München, 80336 Munich, Germany
[3]Transgenic Core Facility, Max Planck Institute of Molecular Cell Biology and Genetics, 01307 Dresden, Germany
[4]Genome Engineering Facility, Max Planck Institute of Molecular Cell Biology and Genetics, 01307 Dresden, Germany
[5]University Cancer Center (UCC) Dresden, Medical Systems Biology, Medizinische Fakultät Carl Gustav Carus, Technische Universität Dresden, 01307 Dresden, Germany and
[6]Institute of Clinical Chemistry and Laboratory Medicine, University Hospital Carl Gustav Carus, Technische Universität Dresden, 01307 Dresden, Germany

Correspondence: Katrin Koehler, PhD, Children's Hospital, Technische Universität, Dresden, Fetscherstrasse 74, D-01307 Dresden, Germany. Email: katrin.koehler@uniklinikum-dresden.de

Abstract

Steroid 21-hydroxylase is an enzyme of the steroid pathway that is involved in the biosynthesis of cortisol and aldosterone by hydroxylation of 17α-hydroxyprogesterone and progesterone at the C21 position. Mutations in *CYP21A2*, the gene encoding 21-hydroxylase, cause the most frequent form of the autosomal recessive disorder congenital adrenal hyperplasia (CAH). In this study, we generated a humanized 21-hydroxylase mouse model as the first step to the generation of mutant mice with different CAH-causing mutations. We replaced the mouse *Cyp21a1* gene with the human *CYP21A2* gene using homologous recombination in combination with CRISPR/Cas9 technique. The aim of this study was to characterize the new humanized mouse model. All results described are related to the homozygous animals in comparison with wild-type mice. We show analogous expression patterns of human 21-hydroxylase by the murine promoter and regulatory elements in comparison to murine 21-hydroxylase in wild-type animals. As expected, no *Cyp21a1* transcript was detected in homozygous *CYP21A2* adrenal glands. Alterations in adrenal gene expression were observed for *Cyp11a1*, *Star*, and *Cyb11b1*. These differences, however, were not pathological. Outward appearance, viability, growth, and fertility were not affected in the humanized *CYP21A2* mice. Plasma steroid levels of corticosterone and aldosterone showed no pathological reduction. In addition, adrenal gland morphology and zonation were similar in both the humanized and the wild-type mice. In conclusion, humanized homozygous *CYP21A2* mice developed normally and showed no differences in histological analyses, no reduction in adrenal and gonadal gene expression, or in plasma steroids in comparison with wild-type littermates.

Key Words: 21-hydroxylase, *CYP21A2*, *Cyp21a1*, congenital adrenal hyperplasia, CAH, humanized mouse model

Abbreviations: ACTH, adrenocorticotropic hormone; CAH, congenital adrenal hyperplasia; HDR, homology-directed repair; H&E, hematoxylin and eosin; HPA, hypothalamic-pituitary-adrenal; LC-MS/MS, liquid chromatography–tandem mass spectrometry; PBS, phosphate-buffered saline; PCR, polymerase chain reaction; POR, cytochrome P450 oxidoreductase; SF-1, steroidogenic factor-1; StAR, steroidogenic acute regulatory protein; TH, tyrosine hydroxylase; WT, wild-type.

Steroid 21-hydroxylase is a cytochrome P450 enzyme that catalyzes the hydroxylation of the adrenal steroid hormones progesterone and 17-hydroxyprogesterone at the C21 position of the steroid biomolecules [1]. It is involved in the biosynthesis of 11-deoxycortisol and deoxycorticosterone, the precursors of the glucocorticoid cortisol and the mineralocorticoid aldo-sterone, respectively. Steroid 21-hydroxylase is localized in endoplasmic reticulum membranes of the adrenal cortex. The human steroid 21-hydroxylase consists of 495 amino acids with a molecular weight of 52 kDa [2, 3]. The encoding human *CYP21A2* gene (MIM*613815) is located at chromosome 6p21.3, spans 3.35 kb, and consists of 10 exons [2, 4]. Homozygous or compound heterozygous mutations in *CYP21A2* are the most common cause of congenital adrenal hyperplasia (CAH). A blockade in the steroid biosynthesis pathway leads to an excessive accumulation of steroid precursors, which are converted into adrenal androgens, resulting in an excess of androgens. In female patients with the classic (severe) form of CAH, adrenal androgen excess causes prenatal virilization of the external genitalia. Patients of both sexes have an increased risk for life-threatening adrenal crises throughout their entire life [5]. The lack of cortisol leads to increased adrenocorticotropic hormone (ACTH) secretion by the pituitary gland due to the lack of negative feedback regulation of the hypothalamic-pituitary-adrenal (HPA) axis. Elevated ACTH levels stimulate adrenal growth resulting in adrenal hyperplasia.

The pseudogene (*CYP21A1P*) is located 30 kb downstream from the functional *CYP21A2* gene and has 98% exonic

Received: 15 December 2021. **Editorial Decision:** 7 April 2022. **Corrected and Typeset:** 12 May 2022

sequence identity and 96% intronic homology to functional *CYP21A2* [2, 4]. Although the pseudogene is not functional, it plays a crucial role in the frequency of changes in *CYP21A2*. Mutations in the pseudogene are often transferred to the functional gene by microconversion events. Intergenic recombinations with the pseudogene are responsible for more than 90% of *CYP21A2* mutations associated with 21-hydroxylase deficiency [6, 7]. In the mouse genome, *Cyp21a1* is the functional gene and *Cyp21a2-p* is the pseudogene [8, 9]. The murine and human 21-hydroxylase genes show a high level of homology, with 77.5% DNA identity and 72.5% identity on the protein level (HomoloGene—NCBI, 2021). In addition, both genes are located in the same region within the class III region of the major histocompatibility complex in both species (Fig. 1) [10].

The first rodent model for 21-hydroxylase deficiency was the H-2aw18 mouse strain [11]. Extensive genetic analysis verified complex gene rearrangement due to an unequal crossing over, which generates a mutant *Cyp21a2-p-Cyp21a1* hybrid gene [9]. Unfortunately, these mice die at an early postnatal stage [9, 11, 12]. This lethality can be mitigated by intensive dexamethasone treatment of dams and pups, but the mouse model remains difficult to handle [12]. Another animal model for human CAH is the *Cyp11b1* knock-out mouse. These mice exhibit glucocorticoid deficiency, mineralocorticoide excess, adrenal hyperplasia, mild hypertension, and hypokalemia [13]. Although useful in studying CAH, none of the existing mouse models can be used to test the efficacy of molecules interacting with human CYP21A2 protein for CAH drug development. Therefore, the development of a mouse model with the human *CYP21A2* gene is of particular importance.

In this study, we generated and characterized a humanized *CYP21A2* mouse model with the aim of investigating the effects of CAH-causing mutations in the future. We show that the human 21-hydroxylase enzyme completely replaces the function of the mouse enzyme without reducing the steroid hormone levels, viability, growth, and fertility. This mouse model is therefore an excellent animal model for further studies and for introducing human point mutations to develop novel humanized CAH mouse models.

Materials and Methods

Experimental Animals

All animal experiments were conducted in accordance with accepted standards of animal care as outlined in the Ethical Guidelines of the German Animal Welfare Act and the Directive 2010/63/EU for the protection of animals used for scientific purposes. C57Bl/6NCrl mice were purchased from Charles River (Sulzfeld, Germany). Chimeras and founder *CYP21A2* heterozygous mice were generated and bred on a C57Bl/6NCrl genetic background. Breeding and maintenance of *CYP21A2* homozygous, heterozygous, and wild-type animals were done at the mouse facility of the Center for Regenerative Therapies Dresden (CRTD), Technische Universität Dresden, Germany. All mice were housed under specific pathogen-free conditions in individually ventilated cages on a 12-hour day/night cycle with free access to food and water. All animal procedures were performed according to institutional guidelines and in accordance with the state authorities (Landesdirektion Sachsen). The stress assessment of the genetically altered line was carried out according to the protocols of the Federal Institute for Risk Assessment (BfR) (https://www.bfr.bund.de/cm/343/beurteilung-der-belastung-genetisch-veraenderter-maeuse-und-ratten-version-2.pdf). The animal experiments were approved by the ethical and research board of the Regierungspräsidium Dresden (reference AZ: 25-5131/449/37—TVV 35/2018).

Generation of Transgenic CYP21A2 Mice C57Bl/6NCrl-Cyp21a1$^{tg(CYP21A2)Koe}$

Humanized *CYP21A2* mice were generated by replacing the 2620-bp *Cyp21a1* mouse gDNA sequence with the orthologous 2713-bp *CYP21A2* human gDNA sequence using CRISPR/Cas9-mediated gene targeting. RNA guides were designed using Geneious software and the CRISPOR online tool (http://crispor.tefor.net/) and purchased as crRNA (Integrated DNA Technologies Germany GmbH). Gene targeting was performed in mouse embryonic stem (mES) cells JM8A1.N3 (from C57Bl/6NTacBom, Taconic) using the guide crRNAs 5′-TGTGGGGCCAATGGAAGCTC-3′ (5′ side of *Cyp21a1*) and 5′-GTGAGCGTCCTTGACAGGAT-3′ (3′ side of *Cyp21a1*) and a homology-directed repair (HDR) donor plasmid pUC57 (GenScript) containing fully humanized *CYP21A2* sequence (both exons and introns) flanked by

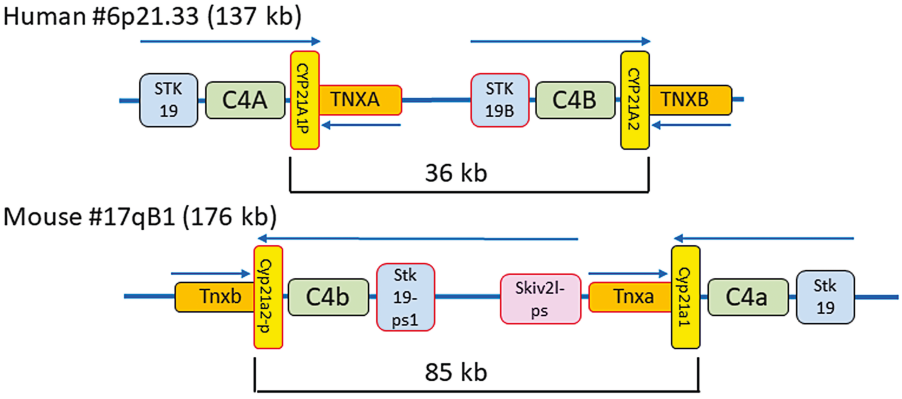

Figure 1. Schematic diagram of the gene locus of human and mouse 21-hydroxylase. The *CYP21A2/Cyp21a1* gene and its related pseudogene *CYP21A1P/Cyp21a2-p* are located in the major histocompatibility (MHC) locus neighboring 3 other genes which are serine/threonine kinase 19 (*STK19/Stk19*), complement *C4A/C4a* and *C4B/C4b* as well as tenascin-X A and B (*TNXA/B, Tnxa/b*). The mouse locus on chromosome 17 have the same gene duplication cassette as the human locus on chromosome 6 except the extra pseudogene superkiller viralicidic activity 2-like (*Skiv2l-ps1*). Pseudogenes are framed in red. Arrows mark the reading direction of the genes.

1000 bp 5′ and 3′ *Cyp21a1* mouse homology arms. The construct contains several silent point mutations in *CYP21A2* to create protospacer adjacent motif (PAM) sequences at the sites where specific point mutations will be inserted in the future. A BamHI restriction site was added in intron 7 to allow restriction-ligation cloning of the loxP-site flanked PGK-NeoR selection cassette. The Cas9, guide RNAs, and HDR donor were electroporated into mES cells using a Neon Transfection System (Thermo Fischer). Forty-eight hours after electroporation, mES cells were selected with G418. Genomic DNA from resistant colonies was tested for correct replacement of the mouse *Cyp21a1* by the human *CYP21A2* gene with 2 polymerase chain reaction (PCR) using primers located upstream of the 5′ and downstream of the 3′ homologous region in combination with one internal primer each (5′-CAGGTAGAGCAGATGACTAG-3′ with 5′-CAATGGTCCTCTTGGAGTTC-3′ and 5′-GTGTCATCCTCAAGATGCAG-3′ with 5′-CTCTGGGGTTTGAATTGGG-3′). Positive clones were PCR-verified for exclusion of random integration of the donor plasmid backbone with ampicillin sequence-specific primers. Correct clones were introduced into C57Bl/6NCrl 8-cell stage embryos by laser-assisted ES-cell injection followed by transfer into pseudopregnant donor mice. Germ line transmission was obtained by mating male chimeras with C57Bl/6NCrl wild-type females. Genotypes were determined by multiplex PCR using the following primers: for the wild-type allele, forward primer (5′-CCAAGACCAGGGTGAGCGT-3′); for the CYP21A2 allele, forward primer (5′-GTGTCATCCTCAAGATGCAG-3′) in combination with reverse primer (5′-CTCACACCCCAGTAGAGAAG-3′) for both alleles. Animals carrying the *CYP21A2* allele were crossbred with Cre-deleter mice (PGK-Cre [N]). Resulting offspring that no longer carried the selection cassette in intron 7 were then intercrossed to generate homozygous *CYP21A2* mice (see Fig. 2).

Blood Pressure Measurement

Under light isoflurane (0.5%) anesthesia, blood pressure was recorded by the tail-cuff method as described previously [14], using the NIBP System for mice (ADInstruments, Oxford, UK) connected to a PowerLab 4/16 system.

Mouse Specimen Collection

100 µL blood was collected from 4-week and 8-week-old mice from the retrobulbar venous plexus into a heparin tube and the plasma separated and stored at −80 °C for further analysis. At an age of 10 weeks, mice were anesthetized intraperitoneally with ketamine-xylazine solution followed by a final cardiac puncture for blood collection. Cervical dislocation was used to ensure euthanasia after bleeding out. Adrenal glands, testis, and ovaries were harvested and grossly examined. All organs were snap-frozen in liquid nitrogen for gene expression and kept at −80 °C before analysis or fixed in 4% neutral-buffered formalin for histology.

Plasma Steroid and ACTH Measurement

Plasma steroid levels were determined by liquid chromatography–tandem mass spectrometry (LC-MS/MS) as previously described [15]. ACTH levels were evaluated in mouse plasma by luminescent immunoassay kit (Siemens Healthcare Diagnostics Cat# LKAC1, RRID:AB_2909441, https://scicrunch.org/scicrunch/data/source/nif-0000-07730-1/search?q=AB_2909441&l=AB_2909441) at IMMULITE 1000 system according to the manufacturer's protocol.

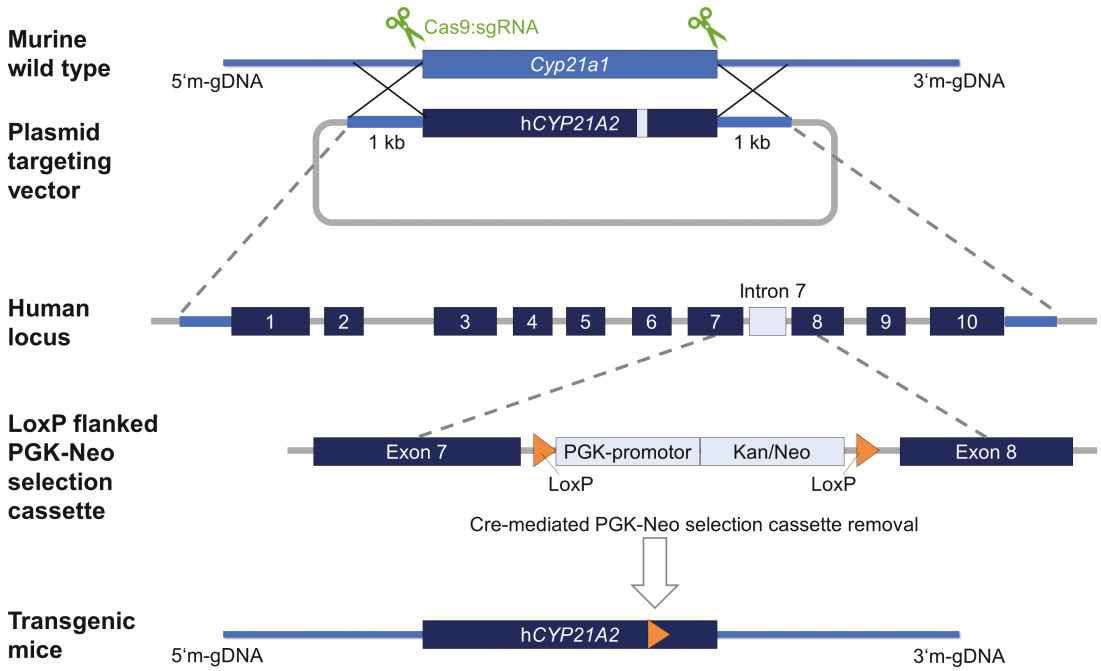

Figure 2. Generation of the transgenic CYP21A2 mouse model. Schematic presentation of homologous recombination of the targeting vector carrying the human *CYP21A2* sequence (dark blue) flanked by 1 kb mouse homology arms (light blue), with the endogenous *Cyp21a1* gene locus (light blue): wild-type *Cyp21a1* gene locus (top), targeting HDR donor plasmid containing fully humanized *CYP21A2* sequence and a PGK-Neo selection cassette flanked by LoxP sites (middle with twice zoom-in), and transgenic gene locus (bottom) after homologous recombination and LoxP sites excision by Cre recombinase, leaving a single LoxP as a genomic scar.

Histological Analysis

Two pairs of male and female wild-type (n = 4: 2 male, 2 female) and *CYP21A2* homozygous mice (n = 4: 2 male, 2 female) were sacrificed to obtain different organs for tissue sections. After dissection, all tissues were fixed in 4% formaldehyde overnight and embedded in paraffin at the Histology Facility of the BIOTEC Dresden, Germany. Four-micrometer sections of paraffin-embedded mouse adrenal, ovary, and testis specimens were placed on glass slides and stained with hematoxylin and eosin (H&E). Images were captured on a Keyence BZ-X700 microscope (Keyence Corporation of America, Itasca, USA) using identical camera settings and analyzed for histological appearance.

Immunohistochemical Analysis

For immunohistochemistry (IHC), 4-µm sections of paraffin-embedded tissues were dewaxed and treated with citrate buffer for 30 minutes in a microwave oven to demask the binding sites. After washing with phosphate-buffered saline (PBS), tissues were treated with 3% H_2O_2 in methanol for 15 minutes to quench endogenous oxidases. Tissue sections were blocked with 3% normal goat serum, 0.1% bovine serum albumin, and 0.3% Triton X in PBS for 1 hour and probed with the primary antibody rabbit anti-human CYP21A2 (Sigma-Aldrich Cat# HPA053371, RRID:AB_2682131, 1:2500, https://antibodyregistry.org/search.php?q=AB_2682131 in blocking buffer) at 4 °C overnight. After washing with PBS, the sections were incubated with the peroxidase-labeled anti-rabbit secondary antibody using Histofine Simple Stain Mouse MAX PO (Nichirei Biosciences Inc., Tokyo, Japan, Cat# 414341F, RRID:AB_2819094, https://antibodyregistry.org/search?q=AB_2819094) for 30 minutes followed by HistoGreen detection, counterstaining with nuclear fast red and mounted with Pertex mounting medium. The procedure was repeated 2 times with a negative control to confirm the specificity of the staining. Images were made with the Keyence BZ-X700 microscope (Keyence corporation of America, Itasca, USA) followed by colorimetric detection of the antibody signal.

Immunofluorescence Staining

Adrenal glands were fixed (4% PFA, 4 hours), cryoprotected (30% sucrose in PBS, 4 °C overnight), embedded in Tissue-Tek Medium (OCT; Sakura Finetek), and stored at −80 °C. Cryosections were prepared using a CryoStar NX70 Cryostat (Thermo Fisher Scientific) and sliced to 10 µm thickness (Superfrost slides; Thermo Scientific). Sections were then immunostained using specific antibodies against steroidogenic factor-1 (SF-1, rabbit, TransGenic Inc, Cat# KO611, RRID:AB_2861370, https://antibodyregistry.org/search?q=AB_2861370), steroidogenic acute regulatory protein (StAR, rabbit, SantaCruz Biotechnology Cat# sc-25806, RRID:AB_2115937, https://antibodyregistry.org/search?q=AB_2115937), and tyrosine hydroxylase (TH, rabbit, Millipore Cat# AB152, RRID:AB_390204, https://antibodyregistry.org/search?q=AB_390204). Primary antibodies were incubated on sections overnight at 4 °C. Sections were then washed and incubated for 2 hours at room temperature with the secondary antibody (Cy3-goat-anti-rabbit; Jackson ImmunoResearch Labs Cat# 111-165-144, RRID:AB_2338006, https://antibodyregistry.org/search?q=AB_2338006). Nuclei were stained with 4′-6-diamidino-2-phenylindole (DAPI; Thermo Fisher Scientific) and slides were mounted with fluorescent mounting medium (Aqua-Poly/Mount; Polysciences). Fluorescence microscopy was done either with a Zeiss Axio Scan.Z1 widefield slide scanner for whole adrenal scan or with the confocal laser scanning microscope Zeiss LSM 780 (Zeiss, Oberkochen, Germany) and ZEN 3.1 (Zeiss) software.

Total RNA Extraction and Quantitative Reverse Transcription PCR

Total RNA was extracted from mouse adrenal glands, ovaries, and testis (n = 7 of each group) using a NucleoSpin RNA II kit (Macherey-Nagel, Düren, Germany) according to the manufacturer's protocol. Purity of the RNA was assessed using Nanodrop Spectrophotometer (ND-1000) (NanoDrop Technologies, Wilmington, DE, USA). 500 ng of total RNA were reversely transcribed into cDNA using GoScript Reverse Transcription System (Promega, Mannheim, Germany) according to the manufacturer's protocol. Primers for amplification of the specific genes encoding steroidogenic enzymes (*hCYP21A2, Star, Cyp11a1, Cyp17a1, Cyp11b1, Cyp11b2, Hsd3b2*) and of the gene encoding steroidogenic factor-1 (*Nr5a1*) were designed with Primer Express 3.0 and obtained from Eurofins Genomics. A TaqMan Gene Expression Assay was purchased (Mm00487230_g1, ThermoFisher) for analysis of mouse *Cyp21a1*. Real-time PCR was performed using the GoTaq Probe qPCR MasterMix (Promega, Mannheim, Germany) according to the manufacturer's reaction parameters. All samples were assayed in triplicates and quantitative reverse transcriptase PCR was performed using the Quantstudio 5 (Thermo Fisher Scientific Inc.). For sample normalization, the housekeeping gene β-Actin was selected as a reference gene. The delta-delta threshold cycle (ΔΔCt) method was used to determine the fold changes in mRNA expression levels [16].

Statistical Analysis

All data are presented as mean ± SD. All statistical analyses were performed using GraphPad Prism version 6 for Windows (GraphPad Software, La Jolla, CA, USA). Data were analyzed using the Mann-Whitney U test or Student's *t* test with P values ≤ 0.05 considered to be statistically significant for comparison between male and female animals and wild-type control vs transgenic homozygous (h-Hom) line.

Results

Generation of the Humanized CYP21A2 Mouse C57Bl/6NCrl-Cyp21a1$^{tg(CYP21A2)Koe}$

Cas9-mediated genome editing via HDR in mES cells was used to generate humanized mice in which the murine *Cyp21a1* gene has been replaced with the human *CYP21A2* gene (Fig. 2). The mES cells containing *CYP21A2* were screened for correct integration of the human gene and the exclusion of random off-target integrations and subsequently introduced into 8-cell embryo stages by laser-assisted ES-cell injection. Resulting chimeric male mice were mated with C57Bl/6NCrl wild-type (WT) females to produce heterozygous *hCYP21A2* pups. Heterozygous *hCYP21A2* mice were intercrossed with a PGK-Cre deleter strain in order to remove the PGK-Neo-resistance cassette and thus to yield homozygous *hCYP21A2* mice. Hence, the established mouse strain, designated according to the international nomenclature as C57Bl/6NCrl-Cyp21a1$^{tg(CYP21A2)Koe}$ and also referred to as h-Hom, is a humanized *CYP21A2* transgenic mouse line.

h-Hom Mice Show No Alteration in Viability, Growth, and Fertility

The genotype frequencies correspond to Mendelian expectations and are in line with Hardy-Weinberg equilibrium for this mouse population. Intercross of heterozygotes resulted in an approximately 1:2:1 distribution of the genotypes (1.2 WT:2 Het:0.8 Hom; n = 18 litter; litter size 6.7). Homozygous *hCYP21A2* mice (h-Hom) were generally characterized regarding their viability, growth, and fertility and then phenotypically characterized by biochemical and histological analyses. Offspring of h-Hom matings showed no abnormalities in severity assessment of the genetically altered line in the first weeks after birth and had normal litter sizes of an average of 6 pups per litter (range, 4-8 [n = 9]) with a normal sex distribution (46% male, 54% female) and 96.5% survival. The body weight of 10-week-old male and female h-Hom mice were compared with the body weight of 10-week-old WT mice and no significant differences were observed between the 2 animal groups (Fig. 3). Male h-Hom mice had a mean body weight of 26.90 g (± 2.51 g) and WT mice of 25.25 g (± 1.42 g). As expected, male mice were heavier than female mice, which had an average weight of 20.3 g (± 1.83 g) for h-Hom and 21.51 g (± 1.21 g) for WT mice. In the blood pressure measurements of h-Hom and WT females, no significant differences were observed. However, there was noticeable a trend toward higher blood pressure values in h-Hom females compared with WT animals (see Supplementary Figure S1 in [17]).

Effect of Humanization of Cyp21a1 on Steroidogenic Enzyme Expression Levels

The expression of steroidogenic enzymes in the adrenals of 10-week-old mice was analyzed to verify that the expression pattern is retained in h-Hom mice. As expected, h-Hom mice showed no expression of the *Cyp21a1* gene at all (Fig. 4A), while showing *CYP21A2* expression (Fig. 4B). As anticipated, the expression in WT mice was inverse. They showed an adequate *Cyp21a1* expression level, females even higher than males ($P = 0.007$), whereas *CYP21A2* was not expressed. We also analyzed the integrity of the full-length cDNA of *CYP21A2* by reverse transcriptase PCR and proved that the integration of silent point mutations for generation of optimal PAM sites used later for insertion of specific point mutations did not affect the splicing (see Supplementary Figure S2 in [17]). *Cyp11a1* and *Star* were significantly higher expressed in male h-Hom mice compared to male WT animals (p = 0.02) but did not differ in females (Fig. 4C + D). In female mice, only *Cyp11b1* ($P = 0.007$) was higher expressed in h-Hom animals than in WT animals (Fig. 4E). Compared with the other adrenal enzymes, a low gene expression for *Cyp11b2* was observed, which did not differ between groups (Fig. 4F). The same low expression was shown for the gene *Nr5a1,* and the only significant difference was between WT mice, where males had a lower expression than females (Fig. 4H). Gender differences were also seen in the expression of *Cyp11a1*. Male mice, both h-Hom and WT, had a higher expression than female mice. *Star* expression in the h-Hom group was 2-fold higher in males than in females. In contrast, gene expressions of *Cyp11b1* and *Hsd3b2* were significant lower in h-Hom males in comparison with h-Hom females.

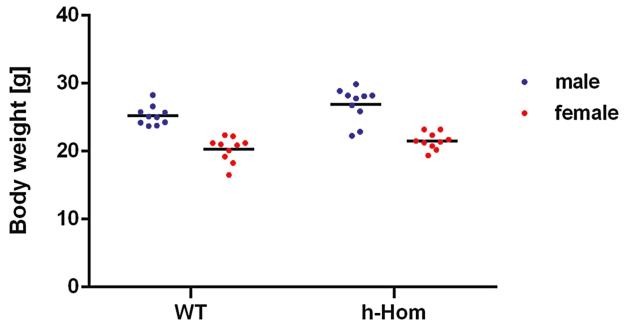

Figure 3. Body weights of 10-weeks old male and female mice. There is no significant difference between WT and h-Hom mice using Student's *t* test. Values represent each data point for one mouse with mean; n = 10.

Ovary gene expression showed no significant differences in female animals of the h-Hom group in comparison with the WT group. The h-Hom and WT mice presented a similar expression pattern for *Cyp17a1*, *Cyp11a1*, *Star,* and *Hsd3b2* (see Supplementary Figure S3 in [17]). The same was seen for the expression of these 4 genes in the male testis (see Supplementary Figure S4 in [17]). As expected, *Cyp17a1* was only detectable in the ovaries and testis, not in the adrenals of mice, while *Cyp21a1*, *Cyp11b1,* and *Cyp11b2* were only detectable in the adrenals, not in the gonads. In general, the investigated gene expressions in the gonads were very low. In addition, *CYP21A2*, similar to *Cyp21a1*, was scarcely expressed neither in h-Hom mouse ovaries nor testis.

Effect of Humanization of Cyp21a1 on Blood Plasma Steroids and ACTH Levels

Steroid plasma measurements were performed on 4-, 8- and 10-week-old male and female mice in both the h-Hom and WT groups (see Supplementary Figure S5 in [17]and Fig. 5). Aldosterone levels at the ages of 4 and 8 weeks showed no significant difference between the 2 groups examined, neither between h-Hom and WT mice nor between male and female (see Supplementary Figure S5 in [17]). However, 12 of the 4-week-old examined mice (n = 31) and 10 of the 8-week-old mice (n = 33) had aldosterone levels below the detection limit because plasma volumes were too low (see Supplementary Figure S5A in [17]). The aldosterone levels of 10-week-old mice were higher than in young animals, with no difference between h-Hom and WT (Fig. 5F). Although the concentrations in WT animals did not differ significantly between male and female (0.38 ± 0.17 ng/mL vs 0.37 ± 0.14 ng/mL), female h-Hom mice had significantly higher aldosterone concentrations than males (0.48 ± 0.18 ng/mL vs 0.29 ± 0.1 ng/mL).

In 4- and 8-week-old mice, h-Hom mice did not differ significantly from the WT group regarding corticosterone levels (see Supplementary Figure S5B in [17]). Compared with younger mice, corticosterone levels were increased with age. In 10-week-old mice, there was a significant difference between female h-Hom and female WT animals ($P = 0.02$) (Fig. 5D). In addition, in both groups (h-Hom and WT), female mice had also significantly higher corticosterone concentrations than male mice.

Blood plasma testosterone concentrations in male mice increased with maturity at the age of 8 weeks in both h-Hom and WT mice. In plasma, 8- and 10-week-old mice had a mean concentration of 3 to 5 ng/mL testosterone, while 4-week-old animals had a mean level of 0.8 ng/mL. No significant difference could be observed between h-Hom and WT groups (see Supplementary Figure S5C in [17] and Fig. 5G).

No additional steroids could be measured in 4- and 8-week-old mice because plasma sample volumes were low,

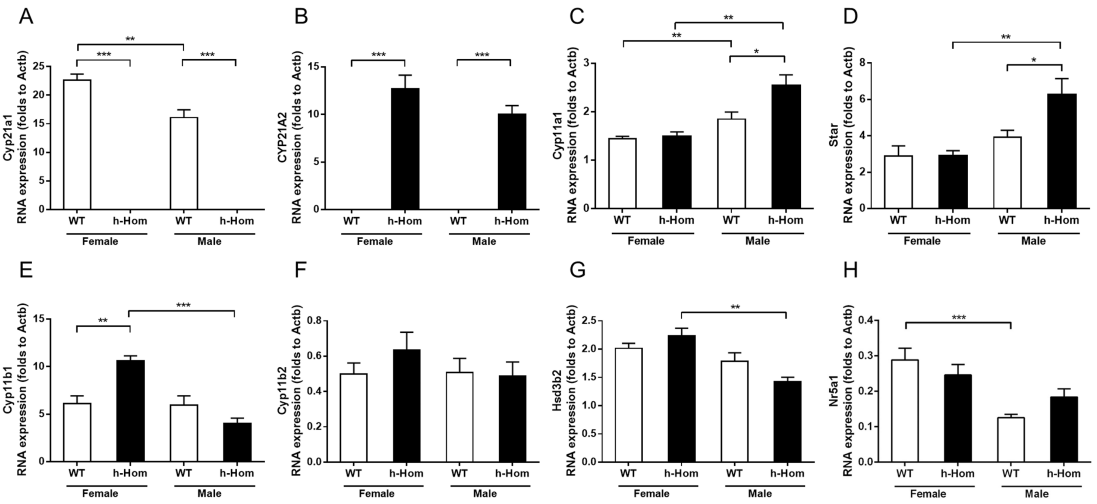

Figure 4. Adrenal gene expression in h-Hom CYP21A2 mice compared to WT mice. Expression of *Cyp21a1* (A), *CYP21A2* (B), *Cyp11a1* (C), *Star* (D), *Cyp11b1* (E), *Cyp11b2* (F), *Hsd3b2* (G) and *Nr5a1* (H) in adrenal glands from male and female 10-wk-old WT and h-Hom mice was determined by qRT-PCR. Relative mRNA expression levels were normalized to β-actin expression (Actb). Experiments were performed in triplicates, and data are expressed as means with SEM. Statistical significance was determined by Mann-Whitney U test, $*P < 0.05$, $**P < 0.01$ and $***P < 0.001$; n = 7.

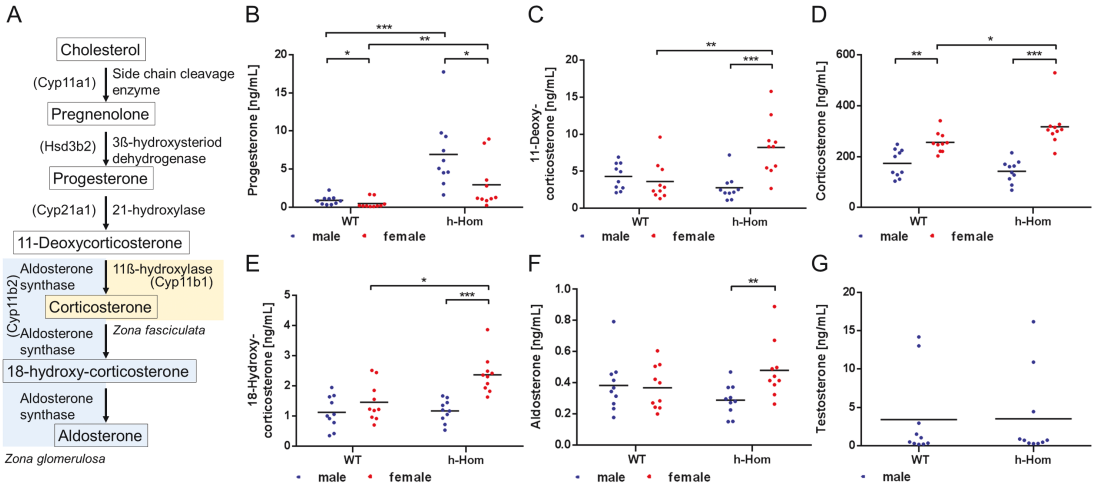

Figure 5. Steroid hormone levels in 10-week-old h-Hom CYP21A2 mice compared with WT mice. Diagram of steroidogenesis pathway in mice (A). Plasma progesterone (B), 11-deoxycorticosterone (C), corticosterone (D), 18OH-corticosterone (E), aldosterone (F), and testosterone (G) levels were determined by LC-MS/MS. Values represent each data point for one mouse (male, blue dots; female, red dots) with mean (black crossbar). Statistical significance was determined by Mann-Whitney U test, $*P < 0.05$, $**P < 0.01$ and $***P < 0.001$; n = 10.

and concentrations were below detection level. However, in the 10-week-old mice, progesterone, 18OH-corticosterone, and 11-deoxycorticosterone levels could be analyzed. The greatest disparity was observed for progesterone levels (Fig. 5B). Both h-Hom males and females showed higher progesterone levels in comparison with WT mice (males $P < 0.001$ and females $P = 0.004$). Moreover, there were significant differences between male and female mice in both the WT and h-Hom groups. Females had significantly lower progesterone concentrations than males.

For 18OH-corticosterone, a significant difference ($P = 0.01$) was seen between female h-Hom group and female WT group (Fig. 5E). However, no difference was found between the 2 male groups. Blood plasma 18OH-corticosterone concentrations of both sexes of h-Hom mice were also significantly different, in that male mice (1.2 ± 0.1 ng/mL) had lower concentrations than female mice (2.4 ± 0.2 ng/mL). Female h-Hom mice had substantially higher 18OH-corticosterone concentrations than all the other groups. Similarly, female h-Hom mice had the highest 11-deoxycorticosterone concentrations (8.2 ± 1.2 ng/mL), which was significantly higher than in female WT mice ($P = 0.009$) and also much higher than in male h-Hom mice ($P = 0.0003$) (Fig. 5C). However, no significant difference was seen between the male groups.

ACTH levels of h-Hom mice (n = 8) varied from 15.1 to 121 pmol/L (mean 61.7 ± 38.4 pmol/L). WT mice had ACTH levels from 16.7 to 59.2 pmol/L (mean 34.9 ± 17.0 pmol/L; n = 8). Compared with the WT mice, the mean ACTH value of the h-Hom was increased nonsignificantly by a factor of 1.77.

Replacement of Cyp21a1 by CYP21A2 Has No Influence on Organ Morphology

Histological investigations were performed to identify abnormalities in morphology and in cell structure of the inner organs of 10-week-old h-Hom *CYP21A2* mice compared with WT mice.

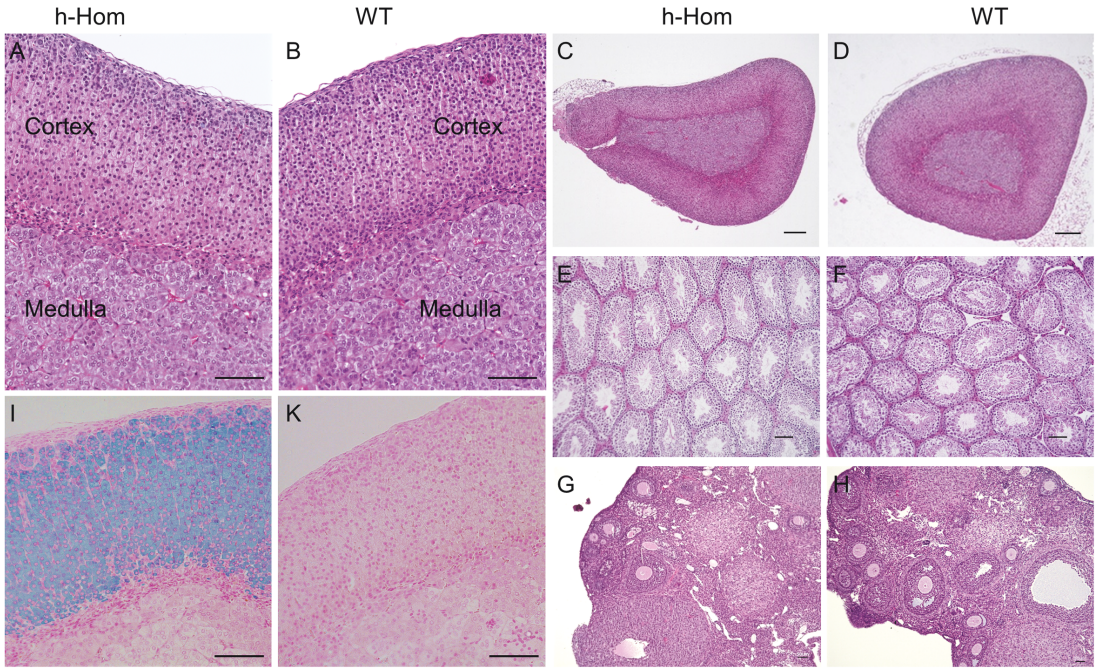

Figure 6. Histological and immunohistochemical staining of organ sections of h-Hom *CYP21A2* mice compared with WT mice at 10 weeks of age. Representative H&E-stained sections of adrenal (A-D), testis (E + F) and ovary (G + H) from h-Hom and WT mice. Representative images of adrenals were obtained from female animals. No gross anatomical differences were observed at low (40×) or high (200×) magnification in h-Hom animals. For specific staining of human CYP21A2, adrenal sections from h-Hom (I) and WT female mice (K) were incubated with anti-human CYP21A2 antibody and visualized by Universal Immuno-peroxidase Polymer method (Nichirei Biosciences Inc.). Note the positively stained cells in the cortex (cyan staining) in the h-Hom mice (I). Cells were counterstained with nuclear fast red staining the nuclei in pink. Scale bar: 50 μm (A,B,E-K) and 200 μM (C-D).

Adrenal gland morphology and zonation of h-Hom mice were similar to WT mice as shown by H&E staining (Fig. 6A-6D). The medulla and cortex of the adrenal could be identified, and no gross histological differences were observed between genotypes. Investigation of medulla specific marker on adrenal cryosections confirmed that the medulla is formed normally in h-Hom mice and that there are no abnormalities and that a sharp border exists between cortex and medulla (Fig. 7A). In addition, immunofluorescence studies were performed to demonstrate protein expression of the steroidogenic enzyme Star and factor Sf-1 in the adrenal glands of genetically engineered mice. No differences were visible between h-Hom and WT sections (Fig. 7B-D).

Morphological comparison of testis and ovaries from h-Hom and WT mice revealed no irregularities assuming a normal development of the humanized mice. Testis from h-Hom and WT males were histologically similar, showing normal seminiferous tubules with spermatozoa in the lumen (Fig. 6E-6F). Ovaries from female h-Hom mice appeared normal, containing numerous follicles in various stages of development as seen in wild-type tissue sections (Fig. 6G-6H).

Immunohistochemical techniques were used to distinguish the humanized adrenals from wild-type adrenals and to verify the correct integration and expression of the human *CYP21A2* gene into the mouse genome. Using an anti-human CYP21A2 antibody, the human 21-hydroxylase was visualized within the adrenal cortex of h-Hom mice (Fig. 6I). As expected, no 21-hydroxylase staining was detectable in the adrenal tissue of WT animals (Fig. 6K). Nuclei and background were counterstained with nuclear fast red, and they had a pink appearance in both h-Hom and WT sections.

Discussion

We established the mouse strain C57Bl/6NCrl-Cyp21a1$^{tg(CYP21A2)Koe}$, which is a humanized *CYP21A2* transgenic mouse line with a targeted replacement of the mouse *Cyp21a1* gene by the human *CYP21A2* gene in mice with a C57Bl/6NCrl genetic background. The aim was to create a model to study the effects of human CAH-causing mutations in the future. In the absence of *Cyp21a1* expression the human *CYP21A2* gene exhibits full gene function. *CYP21A2* expression leads to a humanized 21-hydroxylase and does not grossly affect the synthesis of adrenal steroid hormones. ACTH levels in h-Hom mice were not significantly higher than in WT animals. However, the mean values of WT and h-Hom are in the range of the wild-type sample from the study of Markmann et al, which showed a 4-fold increase of ACTH in 21OH$^{-/-}$ mice [18]. Minor differences in steroid hormone levels are not pathological and range from significant increase of progesterone concentrations in both sexes of the humanized *CYP21A2* transgenic mouse line and significant increase of 11-deoxycorticosterone, corticosterone, and 18-hydroxycorticosterone only in the female mice to nonsignificant changes of aldosterone in comparison with wild-type animals. Consistent with the 7-fold progesterone increase in male h-Hom mice, the enzyme expression of cholesterol side-chain cleavage enzyme (Cyp11a1) and Star is significantly increased in male h-Hom compared with male wild-type animals, whereas all other enzyme expressions

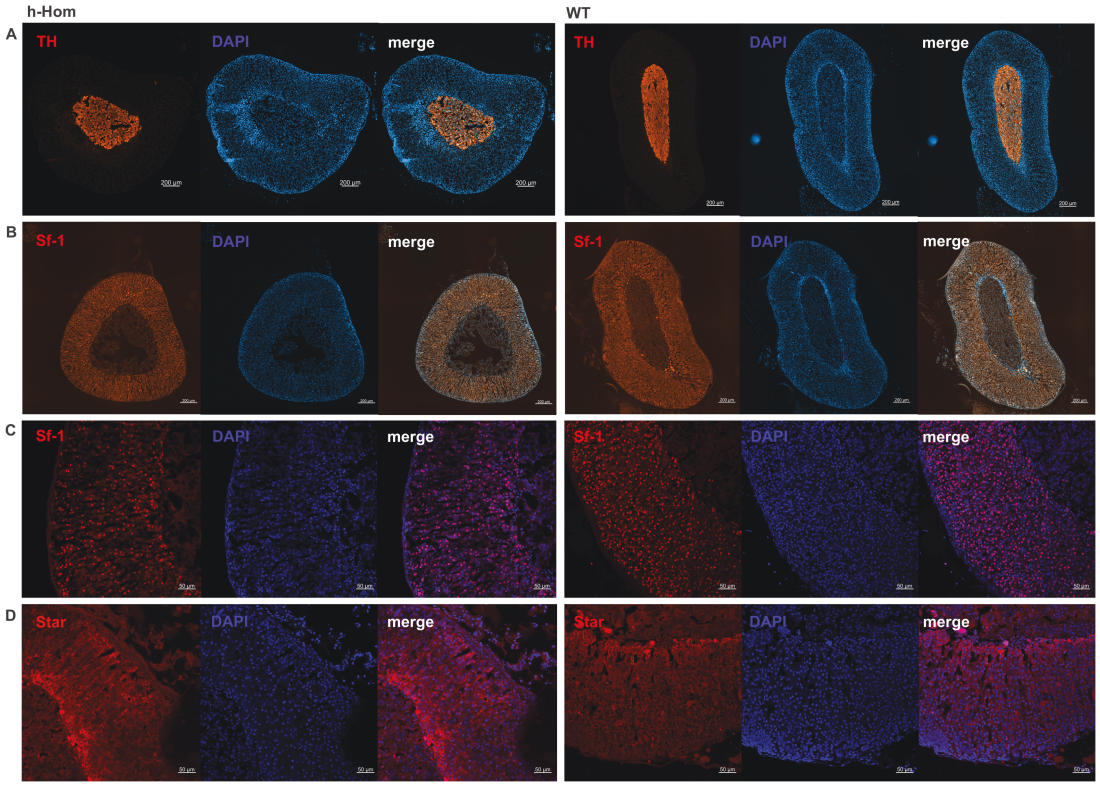

Figure 7. Immunofluorescence staining of cryosections of h-Hom *CYP21A2* mice compared to WT mice. For specific staining adrenal cryosections from h-Hom and WT mice were incubated with anti-tyrosine hydroxylase antibody (A), anti-Sf-1 antibody (B + C) or anti-Star antibody (D) and visualized by a secondary Cy3-fluorescent labeled antibody (red). Nuclei were stained with 4′-6-diamidino-2-phenylindole (DAPI; blue). Scale bar: 200 µM (A, B) and 50 µm (C, D).

measured (Hsd3b2, Cyp11b1, and Cyp11b2) did not change. Star regulates the rate-limiting step in the production of steroid hormones, which is the transfer of cholesterol from the outer to the inner mitochondrial membrane. Cyp11a1 is a mitochondrial enzyme associated with the inner mitochondrial membrane and catalyzes the first reaction in the process of steroidogenesis, the conversion of cholesterol to pregnenolone. The next step from pregnenolone to progesterone is catalyzed by 3beta-hydroxysteroid dehydrogenase (Hsd3b2), which showed no changes in enzyme expression between the groups. However, there was a significant decrease in Hsd3b2 enzyme expression in males compared to females of the h-Hom group, which is in contrast to the higher progesterone levels in the h-Hom males compared to h-Hom females. These findings suggest that not only the level of enzyme expression plays a role for steroid production, but also enzyme activity and the presence of sufficient precursor molecules.

The most prominent difference between h-Hom and WT mice was observed in progesterone levels, in females as well as in males, as plasma progesterone was significantly increased in h-Hom mice. The disparity between h-Hom and WT females could be explained by different estrus cycle phases of the females. In mice, the estrus cycle is divided into 4 phases, proestrus, estrus, metestrus, and diestrus, and repeats every 4 to 5 days [19]. For hormonal analyses, it is substantial to examine female mice being in the same cycle as different phases of the estrus cycle have different impact on the progesterone level in the blood. In a previous study, it was demonstrated that the serum levels of progesterone were highest in metestrus and lowest in diestrus in 3- to 4-month-old female C57BL6 mice [20]. These cyclical changes in serum levels of progesterone could be one explanation for the significant differences between h-Hom and WT females. Therefore, the estrogen levels are important to determine in advance and to identify the stage of estrus cycle should be considered for future studies on these mice.

There is also a sex dimorphism with regard to the effect of the *CYP21A2* transgene on circulating corticosterone and the precursors 11-deoxycorticosterone and 18OH-corticosterone with significant increases only in female h-Hom animals compared with wild-type females, but not in males, which we cannot explain yet. The kinetics of the 21-hydroxylase may play a role. At least the end product corticosterone is not lowered, as would be expected in the case of an enzyme defect. Therefore, no impact on the usefulness of the model for studying the effects of *CYP21A2* mutations is expected.

Corticosterone is the major glucocorticoid in rodents and has the highest blood plasma concentration of all steroids produced by the adrenal gland. It regulates metabolism and has roles in regulating the immune system and stress response. Aldosterone is the major mineralocorticoid; it plays a central role in the regulation of sodium and potassium levels in plasma and is involved in the homeostatic regulation of blood pressure. In our study, most prominent differences in steroid hormone concentrations were measured not between WT and the humanized hom group, but between the male and female mice. This phenomenon is already known. In rodent studies, it has been shown that females have higher circulating corticosterone and ACTH levels than males [21]. Sex hormones in rodents affect the HPA axis at different levels. This includes the activation of gene expression at the hypothalamic

paraventricular nucleus, the regulation of gene expression of the ACTH precursor protein proopiomelanocortin in the anterior pituitary, and a negative feedback role via circulating glucocorticoids in these central organs [22]. Androgen deficiency due to orchiectomy increases basal and stress-induced corticosterone and ACTH levels in the blood, while ovarian resection has the opposite effect [23]. Conversely, sex hormone replacement can reverse these effects [24]. This points to the conclusion that estrogens stimulate the HPA axis while androgens inhibit its activation.

For its catalytic activity, 21-hydroxylase depends on electron transfer from its redox partner cytochrome P450 oxidoreductase (POR). In the presented mouse model human 21-hydroxylase has to interact with mouse POR which could have significant impact on the catalytic activity. However, the conserved domains for interaction with the cytochrome P450 enzymes like NADPH-dependent FMN reductase domain and ferredoxin reductase (FNR) domain are highly conserved between human and mouse POR (Supplementary Figure S6 [17]). *Mus musculus* POR (NP_032924) shows 92% identity (624/678 AA) and 96% positives (653/678 AA) to *Homo sapiens* POR (NP_000932) (Supplementary Figure S6C [17]). Whether the mouse POR influences the catalytic activity of the human 21-hydroxylase in the mouse organism has to be further investigated.

Humanized mice have become important preclinical tools for biomedical research. In the early 2000s, the development of immunodeficient mice bearing mutations in the IL-2 receptor common gamma chain ($IL2rg^{null}$) was a key breakthrough in drug research. Since then, immunodeficient mice engrafted with functional human cells and tissues have become increasingly important as small preclinical animal models for the study of human diseases [25]. Moreover, transgenic mice expressing antibody-coding human gene sequences have proven to be useful for generation of high-affinity human sequence-specific monoclonal antibodies against a wide variety of clinical indications in cancer, autoimmune or inflammatory diseases, and infectious diseases [26]. Despite existing CAH models, the importance of a humanized mouse model for the research of human specific treatment options in CAH is evident, and we aim to support this research with our mouse line.

All in all, the generated humanized *CYP21A2* knock-in mouse model can be utilized to provide additional information on the functional significance of the *CYP21A2* gene. On the basis of clinical information from patients with CAH, these humanized mice can also be useful for translation into the clinic [25, 27]. The future goal is to integrate naturally occurring and clinically relevant mutations that show residual enzyme activity and a phenotype with the simple virilization form of CAH in humans [28]. We therefore will focus in the future on 2 point mutations that cause different severity of symptoms in patients with CAH: (i) c.518T>A p.Ile173Asn, causing a simple virilizing form with lower than 2% enzymatic activity; and (ii) c.1451G>A p.Arg484Gln, which results in a simple virilizing form with 1% to 4% enzymatic activity [29, 30]. With the integration of one of these different mutations into each mouse strain, a viable mouse model is expected based on the residual enzyme activity. Targeted insertion of point mutations can better mimic the clinical phenotypes of affected CAH patients than traditional transgenic mice. Moreover, a careful phenotypic characterization of these different mouse strains, in which an adrenal phenotype might be discovered, can serve as a starting point for further functional analysis [10]. One fact to consider of the future CAH mouse models is that they will not be able to replicate the excessive secretion of androgens observed in CAH patients. In contrast to the human adrenal gland, the mouse adrenal cortex cannot produce androgens (DHEA) because it lacks the enzyme steroid 17α-hydroxylase (Cyp17a1). Thus, androgen production in mice is restricted to the gonads. After the establishment and characterization of the new transgenic mouse models, it is intended to use them further as an in vivo test system for potential treatments of CAH, for example for newly developed antibodies, peptides, and biological active chaperones. Overall, humanized homozygous *CYP21A2* mice are not only a very powerful model to study 21-hydroxylase function and CAH metabolic features, but clinical applications could also be easier to anticipate in the future.

With the characterization of the humanized 21-hydroxylase mouse model, we show that the human 21-hydroxylase replaces the function of the mouse 21-hydroxylase enzyme and catalyzes the sequential step from 11-deoxycorticosterone to corticosterone in the steroidogenic pathway without reducing the steroid hormone levels. Homozygous C57Bl/6NCrl-$Cyp21a1^{tg(CYP21A2)Koe}$ mice did not show any impairment of viability, growth, and fertility. Therefore, they are an excellent model for introducing human point mutations and studying human 21-hydroxylase enzyme activity.

Acknowledgments

We thank Johanna Reppe and the team of the CRTD animal facility for animal care. The excellent technical assistance of Denise Kaden (LC-MS/MS facility) and Susanne Weiche (Histology Facility of the BIOTEC Dresden) is greatly acknowledged. We particularly thank Florian Gembhardt for support with blood pressure measurements as well as Charlotte Steenblock and Uta Lehnert for help with immunofluorescence staining.

Financial Support

This work was supported by the Deutsche Forschungsgemeinschaft (DFG, German Research Foundation) within the CRC/Transregio 205/1 TP A04 to A.H. and N.R. project number: 314061271-TRR 205 and by the Else Kröner-Fresenius-Stiftung and the Eva Luise und Horst Köhler Stiftung within the Clinician Scientist program RISE (2019_KollegSE.03) to FQ. TS was supported by Graduate Academy of the TU Dresden financed by funds from the excellence initiative of the federal and state governments.

Author Contributions

T.S., K.K., N.R., and A.H. conceived and designed the experiments. T.S., K.K., F.Q., S.R.T., D.L., R.N., and I.R. performed experiments. T.S., I.R., and M.P. analyzed and interpreted the data. A.K.H. and M.S. designed the guided RNAs and the target construct. N.R., K.K., and A.H. supervised the study. K.K. and T.S. wrote the manuscript. All authors reviewed and approved the final version of the manuscript.

Potential Conflicts of Interest

All authors declare no conflict of interest.

Data Availability

All data generated or analyzed during this study are included in this published article or are available from the corresponding author on request.

References

1. Miller WL, Auchus RJ. The molecular biology, biochemistry, and physiology of human steroidogenesis and its disorders. *Endocr Rev*. 2011;32(1):81-151. doi:10.1210/er.2010-0013
2. Higashi Y, Yoshioka H, Yamane M, Gotoh O, Fujii-Kuriyama Y. Complete nucleotide sequence of two steroid 21-hydroxylase genes tandemly arranged in human chromosome: a pseudogene and a genuine gene. *Proc Natl Acad Sci USA*. 1986;83(9):2841-2845. doi:10.1073/pnas.83.9.2841
3. Nebert DW, Nelson DR, Coon MJ, *et al*. The P450 superfamily: update on new sequences, gene mapping, and recommended nomenclature. *DNA Cell Biol*. 1991;10(1):1-14. doi:10.1089/dna.1991.10.1
4. White PC, New MI, Dupont B. Structure of human steroid 21-hydroxylase genes. *Proc Natl Acad Sci USA*. 1986;83(14):5111-5115. doi:10.1073/pnas.83.14.5111
5. Reisch N. Substitution therapy in adult patients with congenital adrenal hyperplasia. *Best Pract Res Clin Endocrinol Metab*. 2015;29(1):33-45. doi:10.1016/j.beem.2014.11.002
6. Pignatelli D, Carvalho BL, Palmeiro A, Barros A, Guerreiro SG, Macut D. The Complexities in Genotyping of Congenital Adrenal Hyperplasia: 21-Hydroxylase Deficiency. *Front Endocrinol*. 2019;10:432. doi:10.3389/fendo.2019.00432
7. Narasimhan ML, Khattab A. Genetics of congenital adrenal hyperplasia and genotype-phenotype correlation. *Fertil Steril*. 2019;111(1):24-29. doi:10.1016/j.fertnstert.2018.11.007
8. Parker KL, Chaplin DD, Wong M, Seidman JG, Smith JA, Schimmer BP. Expression of murine 21-hydroxylase in mouse adrenal glands and in transfected Y1 adrenocortical tumor cells. *Proc Natl Acad Sci USA*. 1985;82(23):7860-7864. doi:10.1073/pnas.82.23.7860
9. Riepe FG, Tatzel S, Sippell WG, Pleiss J, Krone N. Congenital adrenal hyperplasia: the molecular basis of 21-hydroxylase deficiency in H-2(aw18) mice. *Endocrinology*. 2005;146(6):2563-2574. doi:10.1210/en.2004-1563
10. Beuschlein F. Animal Models of Adrenal Genetic Disorders. In: *Genetic Steroid Disorders*. Elsevier; 2014:323-329. doi:10.1016/B978-0-12-416006-4.00026-0
11. Gotoh H. [Gene therapy of a lethal mutation associated with adrenal hyperplasia in mice]. *Jikken Dobutsu*. 1993;42(3):279-281.
12. Bornstein SR, Tajima T, Eisenhofer G, Haidan A, Aguilera G. Adrenomedullary function is severely impaired in 21-hydroxylase-deficient mice. *FASEB J Off Publ Fed Am Soc Exp Biol*. 1999;13(10):1185-1194.
13. Mullins LJ, Peter A, Wrobel N, *et al*. Cyp11b1 null mouse, a model of congenital adrenal hyperplasia. *J Biol Chem*. 2009;284(6):3925-3934. doi:10.1074/jbc.M805081200
14. Gembardt F, Bartaun C, Jarzebska N, *et al*. The SGLT2 inhibitor empagliflozin ameliorates early features of diabetic nephropathy in BTBR ob/ob type 2 diabetic mice with and without hypertension. *Am J Physiol Renal Physiol*. 2014;307(3):F317-F325. doi:10.1152/ajprenal.00145.2014
15. Peitzsch M, Dekkers T, Haase M, *et al*. An LC-MS/MS method for steroid profiling during adrenal venous sampling for investigation of primary aldosteronism. *J Steroid Biochem Mol Biol*. 2015;145:75-84. doi:10.1016/j.jsbmb.2014.10.006
16. Schmittgen TD, Livak KJ. Analyzing real-time PCR data by the comparative C(T) method. *Nat Protoc* 2008;3(6):1101-1108. doi:10.1038/nprot.2008.73.
17. Schubert T, Reisch N, Naumann R. Data from: CYP21A2 gene expression in a humanized 21-hydroxylase mouse model does not affect adrenocortical morphology and function. *Open Science Framework*. Deposited March 3, 2022. doi:10.17605/OSF.IO/P3RYQ
18. Markmann S, De BP, Reid J, *et al*. Biology of the Adrenal Gland Cortex Obviates Effective Use of Adeno-Associated Virus Vectors to Treat Hereditary Adrenal Disorders. *Hum Gene Ther*. 2018;29(4):403-412. doi:10.1089/hum.2017.203
19. Allen E. The oestrous cycle in the mouse. *Am J Anat*. 1922;30(3):297-371. doi:10.1002/aja.1000300303
20. Nilsson ME, Vandenput L, T, ivesten Å, *et al*. Measurement of a Comprehensive Sex Steroid Profile in Rodent Serum by High-Sensitive Gas Chromatography-Tandem Mass Spectrometry. *Endocrinology*. 2015;156(7):2492-2502. doi:10.1210/en.2014-1890
21. Heck AL, Handa RJ. Sex differences in the hypothalamic-pituitary-adrenal axis' response to stress: an important role for gonadal hormones. *Neuropsychopharmacol Off Publ Am Coll Neuropsychopharmacol*. 2019;44(1):45-58. doi:10.1038/s41386-018-0167-9
22. Lyraki R, Schedl A. The Sexually Dimorphic Adrenal Cortex: Implications for Adrenal Disease. *Int J Mol Sci*. 2021;22(9):4889. doi:10.3390/ijms22094889
23. Seale JV, Wood SA, Atkinson HC, *et al*. Gonadectomy reverses the sexually diergic patterns of circadian and stress-induced hypothalamic-pituitary-adrenal axis activity in male and female rats. *J Neuroendocrinol*. 2004;16(6):516-524. doi:10.1111/j.1365-2826.2004.01195.x
24. Seale JV, Wood SA, Atkinson HC, Harbuz MS, Lightman SL. Gonadal steroid replacement reverses gonadectomy-induced changes in the corticosterone pulse profile and stress-induced hypothalamic-pituitary-adrenal axis activity of male and female rats. *J Neuroendocrinol*. 2004;16(12):989-998. doi:10.1111/j.1365-2826.2004.01258.x
25. Walsh NC, Kenney LL, Jangalwe S, *et al*. Humanized Mouse Models of Clinical Disease. *Annu Rev Pathol*. 2017;12:187-215. doi:10.1146/annurev-pathol-052016-100332
26. Lonberg N. Human antibodies from transgenic animals. *Nat Biotechnol*. 2005;23(9):1117-1125. doi:10.1038/nbt1135
27. Brehm MA, Shultz LD, Greiner DL. Humanized Mouse Models to Study Human Diseases. *Curr Opin Endocrinol Diabetes Obes*. 2010;17(2):120-125. doi:10.1097/MED.0b013e328337282f
28. Haider S, Islam B, D'Atri V, *et al*. Structure–phenotype correlations of human CYP21A2 mutations in congenital adrenal hyperplasia. *Proc Natl Acad Sci USA*. 2013;110(7):2605-2610. doi:10.1073/pnas.1221133110
29. Tusie-Luna MT, Traktman P, White PC. Determination of functional effects of mutations in the steroid 21-hydroxylase gene (CYP21) using recombinant vaccinia virus. *J Biol Chem*. 1990;265(34):20916-20922
30. Robins T, Bellanne-Chantelot C, Barbaro M, Cabrol S, Wedell A, Lajic S. Characterization of novel missense mutations in CYP21 causing congenital adrenal hyperplasia. *J Mol Med Berl Ger*. 2007;85(3):247-255. doi:10.1007/s00109-006-0121-x